Feedback linearisation in systems with non-smooth nonlinearities

Shakir Jiffri[1], Paolo Paoletti[2] and J. E. Mottershead[3]

School of Engineering, University of Liverpool, Brownlow Hill, Liverpool L69 3GH, UK

This article aims to elucidate the application of feedback linearisation in systems having non-smooth nonlinearities. With the aid of analytical expressions originating from classical feedback linearisation theory, it is demonstrated that for a subset of non-smooth systems ubiquitous in the structural dynamics and vibrations community, the theory holds soundly. Numerical simulations on a three degree of freedom aeroservoelastic system are carried out to illustrate the application of feedback linearisation for a specific control objective, in the presence of dead-zone and piece-wise linear structural nonlinearities in the plant. An in-depth study of the arising zero-dynamics, based on a combination of analytical formulations and numerical simulations, reveals that asymptotically stable equilibria exist, paving the way for the application of feedback linearisation. The latter is demonstrated successfully through pole-placement on the linearised system.

Keywords: nonlinear control, feedback linearisation, non-smooth systems, freeplay, dead-zone, piece-wise linearity, zero-dynamics, non-smooth stability

Nomenclature

$\succ / \prec$ = positive/negative definite

$ker(\square)$ = kernel/null-space function

[1] Postdoctoral Research Associate, Centre for Engineering Dynamics, School of Engineering.
[2] Lecturer, Centre for Engineering Dynamics, School of Engineering.
[3] Professor, Head of the Centre for Engineering Dynamics, School of Engineering.

$K[\square]$	=	Filippov's differential inclusion
$\alpha, \dot{\alpha}$	=	aerofoil pitch deflection, pitch velocity
$\beta, \dot{\beta}$	=	aileron flap deflection, flap velocity
β_{com}	=	commanded flap deflection
$\zeta_\alpha, \zeta_\beta, \zeta_\xi$	=	pitch / flap / plunge mode damping ratio
λ	=	freeplay / piece-wise linear stiffness parameter
μ	=	ratio of mass of aerofoil section and other rotating parts to the mass of a cylinder of air with diameter 2*b*
$\xi, \dot{\xi}$	=	aerofoil plunge displacement, plunge velocity
$\omega_\alpha, \omega_\beta, \omega_\xi$	=	uncoupled pitch / flap / plunge mode natural frequency
a	=	distance from aerofoil mid-chord to rotational axis, normalised by *b*
b	=	aerofoil semi-chord
c	=	distance from aerofoil mid-chord to aileron hinge line, normalised by *b*
$\mathbf{A}, \mathbf{B}$	=	state and input matrices of linearised system
$\hat{\mathbf{A}}, \hat{\mathbf{b}}$	=	matrices pertaining to zero-dynamics
$\mathbf{C}$	=	system damping matrix
$\mathbf{C}_t$	=	total aeroelastic damping matrix (structural + aerodynamic)
$\mathbf{D}, \mathbf{E}_1, \mathbf{E}_2, \mathbf{F}_p$	=	matrices relating to augmented states of aeroelastic model
$\mathbf{e}_2$	=	2nd column of a 3×3 identity matrix
$\mathbf{f}_{nl}$	=	nonlinear force vector
$\underline{\mathbf{f}}(\mathbf{x}), \underline{\mathbf{g}}(\mathbf{x})$	=	functions of the state vector in the nonlinear state-space form
g_α	=	the freeplay/piece-wise linear "gap" on either side of the origin
$\mathbf{g}_\alpha$	=	$g_\alpha \mathbf{e}_2$
$\mathbf{G}$	=	input selection matrix in nonlinear system
K_α	=	pitch structural stiffness

$\mathbf{K}$ = system stiffness matrix

$\mathbf{K}_t$ = total aeroelastic stiffness matrix (structural + aerodynamic)

$\mathbf{M}$ = system inertia matrix

$\mathbf{M}_t$ = total aeroelastic inertia matrix (structural + aerodynamic)

$\mathbf{p}$ = 1st column of a 6×6 identity matrix

$\mathbf{P}$ = Lyapunov matrix used in zero-dynamics stability assessment

$\mathbf{q}, \dot{\mathbf{q}}, \ddot{\mathbf{q}}$ = vectors of aerofoil displacements, velocities and accelerations

$\mathbf{q}_a$ = vector of augmented states of aeroelastic system

r_α, r_β = radius of gyration of aerofoil / aileron, normalised with respect to b

$\mathbf{T}$ = transformation between co-ordinates of nonlinear and linear system

$\mathbf{T}_{pl}$ = transformation between co-ordinates of nonlinear and partially linearised system

$T_1, \cdots, T_{13}$ = Theodorsen functions (Appendix A1)

$u, \bar{u}$ = actual and artificial inputs in closed-loop system

$\mathbf{u}, \bar{\mathbf{u}}$ = vectors of actual and artificial inputs in closed-loop system

U^* = reduced air speed

x_α = centre-of-mass distance of wing+aileron from rotational axis, normalised by b

x_β = centre-of-mass distance of aileron from hinge line, normalised by b

$x_1, \cdots, x_8$ = structural states of aeroelastic system

x_{a_1}, x_{a_2} = augmented states in aeroelastic system

$\mathbf{x}, \dot{\mathbf{x}}$ = state and rate vectors of original nonlinear system

$\mathbf{y}$ = outputs chosen for input-output feedback linearisation

$\mathbf{z}, \dot{\mathbf{z}}$ = state and rate vectors of linear system

$\underset{\sim}{\mathbf{z}}, \dot{\underset{\sim}{\mathbf{z}}}$ = state vector of zero-dynamics

$\underset{\sim}{\mathbf{z}}_{eq}$ = equilibrium point of zero-dynamics

$\hat{\underset{\sim}{\mathbf{z}}}, \dot{\hat{\underset{\sim}{\mathbf{z}}}}$ = state and rate vectors of zero-dynamics with origin shifted with respect to a given equilibrium point

$\mathbf{Z}_{(\hat{\mathbf{b}}^T\mathbf{P})}$ = null-space matrix of $\hat{\mathbf{b}}^T\mathbf{P}$

I. Introduction

FEEDBACK linearisation is a nonlinear control method that has found application in several engineering disciplines, including robotics [1] (computed torque control), chemical engineering [2] and, as will shortly be discussed in more detail, aerospace engineering. Well-known texts such as [3-5] present the method in detail. A requirement for the applicability of feedback linearisation is smoothness of the nonlinear system. With such systems, the mathematics of the procedure is straightforward and an abundance of literature presenting application of the method is widely available. For instance, a series of numerical simulations and experiments was undertaken in [6-12] where feedback linearisation was applied in nonlinear aeroelastic systems with smooth structural nonlinearities.

Non-smooth systems, on the other hand, have received much less attention where feedback linearisation is concerned. Recker *et al*. [13], designed an adaptive controller utilising feedback linearisation for systems with a deadzone. The non-smooth nonlinearity, however, was confined to the input and was not part of the state (the open-loop system was smooth). An extension to this work by Ma and Tao [14] generalised the method for cases of full and partial linearisation with or without relative degree. Sun and Ge [15] formulated a criterion for non-smooth non-regular feedback linearisability, where the inputs were allowed to be non-smooth. Hatipoğlu and Özgüner [16, 17] employed feedback linearisation as an intermediate stage in the control of non-smooth systems, and illustrated the control algorithm through a numerical example featuring a single degree of freedom plant. However, an explanation justifying the use of discontinuous linearising feedback was not provided. Other work relating to control of non-smooth systems is available in more abundance, and includes adaptive control of systems with both input and output nonlinearities as investigated by Tao [18] and Tao and Kokotovic [19] and the work of Lin and Qian [20] on adaptive control of systems having unstable linearisation. In [18, 19] the plant considered was linear, and the controller utilised the adaptive inverse as in Recker *et al*. The open-loop system in [20] was nonlinear and smooth. An adaptive control approach which does not require computation of the dead-zone inverse is presented by Ma and Yang [21]. Zhou and Wen [22] address backstepping and adaptive control of uncertain systems with a variety of non-smooth nonlinearities; a collection of more than 170 related references is provided in their book.

This article is motivated by the need to expound the application of feedback linearisation in systems having non-smooth nonlinearities as part of the plant. The main contributions of this paper are:

(a) the admission of a non-smooth structural nonlinearity associated with the *state* of the plant that will be subjected to feedback linearisation,

(b) analysis of theoretical expressions arising from classical feedback linearisation theory to aid understanding of non-smooth feedback linearisation in this context.

Numerical examples are provided to elucidate all ideas developed. Although the present article places an emphasis on aeroelastic systems in terms of the cited literature and numerical illustrations used, the main principles that will be developed are intended for the general case.

II. Feedback Linearisation

Feedback linearisation is a process whereby a nonlinear system is rendered linear through the application of nonlinear feedback and a co-ordinate transformation [3, 4]. Input-state linearisation results in all states of the nonlinear system being linearised, whereas input-output linearisation seeks to linearise the input-output map only. Both forms may be carried out in single-input-single-output (SISO) or multi-input-multi-output (MIMO) configurations. The present article focuses on input-output linearisation of control-affine nonlinear systems, often expressed as

$$\dot{\mathbf{x}} = \underline{\mathbf{f}}(\mathbf{x}) + \underline{\mathbf{g}}(\mathbf{x})u, \qquad u = \alpha(\mathbf{x}) + \beta(\mathbf{x})\bar{u}, \qquad \mathbf{z} = \mathbf{T}(\mathbf{x}), \tag{1}$$

where $u, \bar{u}$ and $\mathbf{T}$ are the nonlinear feedback, artificial input corresponding to the linearised system and co-ordinate transformation respectively. In the general case, the terms $\underline{\mathbf{f}}, \underline{\mathbf{g}}$ in eq. (1) are required to be smooth; the smoothness of $\underline{\mathbf{f}}$ translates to continuous differentiability of the transformation $\mathbf{T}(\mathbf{x})$. The latter is a required condition for the applicability of feedback linearisation, in the general case of eq. (1). However, it will be shown in this paper that for a subset of all systems described by this equation the smoothness condition on $\underline{\mathbf{f}}$ may be relaxed, allowing application of feedback linearisation in a configuration that will be of great utility in a practical context.

A. Second-order nonlinear dynamical systems with displacement outputs

In this article, second-order nonlinear dynamical systems of the form

$$\mathbf{M}\ddot{\mathbf{q}} + \mathbf{C}\dot{\mathbf{q}} + \mathbf{K}\mathbf{q} + \mathbf{f}_{nl}\left(\mathbf{q}, \dot{\mathbf{q}}\right) = \mathbf{G}\mathbf{u} \tag{2}$$

are addressed. This forms a subset of eq. (1), which covers a broad range of elasto-mechanical and aeroelastic vibrations problems encountered in engineering applications. The state-space form of eq. (2) has the structure

$$\begin{Bmatrix} \dot{\mathbf{q}} \\ \ddot{\mathbf{q}} \end{Bmatrix} = \begin{Bmatrix} \dot{\mathbf{q}} \\ \boldsymbol{\Psi}\mathbf{q} + \boldsymbol{\Phi}\dot{\mathbf{q}} + \boldsymbol{\Omega}\mathbf{f}_{nl} \end{Bmatrix} + \begin{bmatrix} \mathbf{0} \\ \boldsymbol{\Pi} \end{bmatrix}\mathbf{u}, \qquad \boldsymbol{\Psi} = -\mathbf{M}^{-1}\mathbf{K}, \quad \boldsymbol{\Phi} = -\mathbf{M}^{-1}\mathbf{C}, \quad \boldsymbol{\Omega} = -\mathbf{M}^{-1}, \quad \boldsymbol{\Pi} = \mathbf{M}^{-1}\mathbf{G}, \tag{3}$$

Comparing the above equation with eq. (1), it is seen that the function $\underline{\mathbf{g}}$ is now constant. Notice that the nature of the nonlinearity as expressed by the term $\mathbf{f}_{nl}$, which may depend on any of the system's states (including displacements and/or velocities), will govern the smoothness properties of $\underline{\mathbf{f}}$ in eq. (1). Input-output feedback linearisation may be carried out by choosing as the output any entry in $\mathbf{q}$ (i.e. any displacement co-ordinate) or a linear combination of its entries.

1 Complete input-output linearisation

The case where the number of inputs and outputs is equal to the number of system degrees of freedom, *n*, is now considered. For simplicity, here one assumes that the number of states in the system is equal to twice the number of degrees of freedom (as in eq. (3)), although this assumption can be relaxed as illustrated in section III. Choosing as the output the entire vector of displacements, i.e. $\mathbf{y} = \mathbf{q}$ and implementing input-output linearisation with each output in turn from $j = 1:n$,

$$\begin{aligned} z_{2j-1} &= y_j = q_j = x_j, \\ z_{2j} &= \dot{y}_j = \dot{q}_j = x_{n+j}, \end{aligned} \qquad \begin{Bmatrix} \dot{z}_{2j-1} \\ \dot{z}_{2j} \end{Bmatrix} = \begin{bmatrix} 0 & 1 \\ 0 & 0 \end{bmatrix}\begin{Bmatrix} z_{2j-1} \\ z_{2j} \end{Bmatrix} + \begin{bmatrix} 0 \\ 1 \end{bmatrix}\bar{u}_j, \qquad \bar{u}_j = \underline{\mathbf{f}}_{(n+j)} + \boldsymbol{\Pi}_{(j,:)}\mathbf{u}, \tag{4}$$

the $2n \times 2n$ transformation $\mathbf{T}$, linear dynamics and nonlinear input may be obtained respectively as

$$\mathbf{z} = \mathbf{T}\mathbf{x}, \quad \mathbf{T}_{(2j-1,\,j)} = \mathbf{T}_{(2j,\,n+j)} = 1, \quad j = 1:n, \quad \text{remaining entries equal to 0,}$$

$$\dot{\mathbf{z}} = \mathbf{A}\mathbf{z} + \mathbf{B}\bar{\mathbf{u}}, \quad \mathbf{A}_{(2j-1,\,2j)} = 1, \quad j = 1:n, \quad \text{remaining entries equal to 0,} \tag{5}$$

$$\mathbf{B}_{(2j,\,j)} = 1, \quad \text{remaining entries equal to 0,}$$

$$\mathbf{u} = \mathbf{\Pi}^{-1}\left(\bar{\mathbf{u}} - \underline{\mathbf{f}}_{(n+1:2n)}\right).$$

It is evident that complete MIMO input-output linearisation has resulted in all states of the system being linearised. The transformation $\mathbf{T}$ is linear, full-rank and independent of the state variables. Furthermore, note that the linear system consists of *n* decoupled subsystems of dimension 2, each involving the displacement and velocity pertaining to a given degree of freedom.

2 Partial input-output linearisation

The case where the equal number of inputs and outputs m is less than the number of system degrees of freedom n is now considered. Applying input-output linearisation as before for m displacement outputs results in the same set of equations as in eq. (4) above, where now $j = 1:m$. This results in only a partial linearisation of the original nonlinear system, viz., $\mathbf{z}_{(1:2m)} = \mathbf{T}_{pl}\mathbf{x}$. The partially linearised system will comprise $2m$ states, leaving a remainder of $2(n-m)$ states unobservable from the outputs. The procedure for investigating stability of this so-called *internal dynamics* is to examine the *zero-dynamics* of the system [3, 4], which requires expressions for the remaining co-ordinates $\mathbf{z}_{(2m+1:2n)}$. These may be chosen arbitrarily provided that the overall transformation $\mathbf{T}$ is non-singular and the dynamics associated with the additional co-ordinates are orthogonal to $\underline{\mathbf{g}}$. The latter condition ensures that the internal dynamics are obtained in the *normal form*, where the system inputs do not appear. The conditions mentioned here are satisfied by a $\mathbf{T}$ having the following structure:

$$\mathbf{z} = \mathbf{T}\mathbf{x} \;\Rightarrow\; \left\{ \begin{array}{c} \mathbf{z}_{(1:2m)} \\ \hline \mathbf{z}_{(2m+1:2n)} \end{array} \right\} = \left[\begin{array}{c|c|c} \multicolumn{3}{c}{\mathbf{T}_{pl}\ \{2m \times 2n\}} \\ \hline \mathbf{0}\left\{(n-m)\times m\right\} & \mathbf{I}\left\{(n-m)\times(n-m)\right\} & \mathbf{0}\left\{(n-m)\times n\right\} \\ \hline \multicolumn{2}{c|}{\mathbf{0}\left\{(n-m)\times n\right\}} & ker(\mathbf{\Pi})\left\{(n-m)\times n\right\} \end{array} \right] \mathbf{x},$$

$$\mathbf{T}_{pl(2j-1,\,j)} = \mathbf{T}_{pl(2j,\,n+j)} = 1, \quad j = 1:m, \quad \text{remaining entries equal to 0,} \tag{6}$$

$$\mathbf{\Pi} \cdot ker(\mathbf{\Pi}) = \mathbf{0}.$$

The dimensions of each block are given in the curly brackets, and *ker* denotes the kernel (null-space) function. It can be verified from the above structure that the linear transformation $\mathbf{T}$ is non-singular and independent of the state variables, and therefore satisfies the conditions of a diffeomorphism, namely that the transformation is continuously differentiable and has a continuously differentiable inverse [4].

B. Feedback Linearisation - Non-smooth Nonlinearities

The case where the nonlinear forcing term $\mathbf{f}_{nl}$ is non-smooth is now considered. A special feature evident in eq. (3) is that the velocity terms $\dot{\mathbf{q}}$ do not involve $\mathbf{f}_{nl}$ and are therefore not explicitly dependent upon non-smooth terms. This special feature contributes to the co-ordinate transformation between linear and nonlinear co-ordinates being constant and non-singular as shown in section II.A.1 and section II.A.2 above. Thus, the nature of the transformation is unaffected by whether the nonlinearity is smooth or not. In conclusion, one can obtain a valid transformation $\mathbf{T}$ that is a diffeomorphism when the nonlinearity is non-smooth or even discontinuous. The behaviour described here is not necessarily true in the general case (e.g. see Appendix A2).

The nature of the dynamics of the linear system resulting from the application of feedback linearisation is now considered. The displacements and velocities of the system are obtained as time-integrals of the velocities and accelerations respectively. Thus, if the non-smooth nonlinearity is continuous, all state variables of the resulting linear system will be smooth, whereas if it is discontinuous, the desired linear system will have smooth displacements and non-smooth but continuous velocities. A direct consequence of this is that the desired linear system resulting from feedback linearisation will take on the nature of the non-smooth nonlinearity. In the case of complete input-output linearisation, this situation is avoided, as the input is designed to cancel all open-loop dynamics as expressed in eq. (4). However, this is indeed applicable to the partial input-output linearisation

case, where the internal dynamics will be governed by the nonlinearity which is not completely eliminated. Thus, if the nonlinearity is non-smooth or discontinuous, one would expect the overall dynamics of the closed-loop system to exhibit some non-smoothness or discontinuity respectively, until the stable internal dynamics have decayed.

III. Numerical model - System Dynamics and Feedback Linearisation

In this work, an aeroservoelastic state-space model with a non-smooth structural nonlinearity – namely piece-wise linearity – has been employed for illustrative purposes. In addition to a general case of piece-wise linearity, the special case of freeplay is also addressed. Numerical simulations aim to demonstrate the ideas established in the preceding section. The state-space form of the model is now presented, with detailed expressions for all system matrices given in Appendix A1.

A. Linear state-space model of aeroservoelastic system

The base model used is that developed by Edwards et al. [23], featuring an approximation of the general unsteady Theodorsen aerodynamics [24] through the use of augmented aerodynamic states. This model comprises a total of 8 states in the first-order state-space representation. Six of these are structural states, namely normalised plunge, pitch, aileron flap (ξ, α, β respectively) and their time-derivatives ($\dot{\xi}, \dot{\alpha}, \dot{\beta}$ respectively). The normalisation of plunge is with respect to the semi-chord *b*. The remaining two states are the augmented aerodynamic states mentioned above (x_{a_1}, x_{a_2}). Equations of motion for the model are given as

$$\dot{\mathbf{x}} = \mathbf{A}\mathbf{x} + \mathbf{B}u, \quad \text{where} \quad u = \beta_{com}, \quad \mathbf{x} = \left\{x_1 \quad x_2 \quad \cdots \quad x_8\right\}^T = \left\{\mathbf{q} \quad \dot{\mathbf{q}} \quad \mathbf{q}_a\right\}^T,$$

$$\mathbf{q} = \left\{\xi \quad \alpha \quad \beta\right\}^T, \qquad \dot{\mathbf{q}} = \left\{\dot{\xi} \quad \dot{\alpha} \quad \dot{\beta}\right\}^T, \qquad \mathbf{q}_a = \left\{x_{a_1} \quad x_{a_2}\right\}^T, \tag{7}$$

$$\mathbf{A} = \begin{bmatrix} \mathbf{0}_{(3\times3)} & \mathbf{I}_{(3\times3)} & \mathbf{0}_{(3\times2)} \\ -\mathbf{M}_t^{-1}\mathbf{K}_t & -\mathbf{M}_t^{-1}\mathbf{C}_t & \mathbf{M}_t^{-1}\mathbf{D} \\ \mathbf{E}_1 & \mathbf{E}_2 & \mathbf{F}_p \end{bmatrix}, \qquad \mathbf{B} = \begin{bmatrix} \mathbf{0}_{(3\times1)} \\ \mathbf{M}_t^{-1}\mathbf{G} \\ \mathbf{0}_{(2\times1)} \end{bmatrix}, \qquad \mathbf{G} = \begin{Bmatrix} 0 \\ 0 \\ r_\beta^2\omega_\beta^2 \end{Bmatrix}.$$

The input in the above equation is the desired flap angle of the aileron.

Fig. 1 depicts the displacement co-ordinates and also various aeroelastic parameters that will be introduced later.

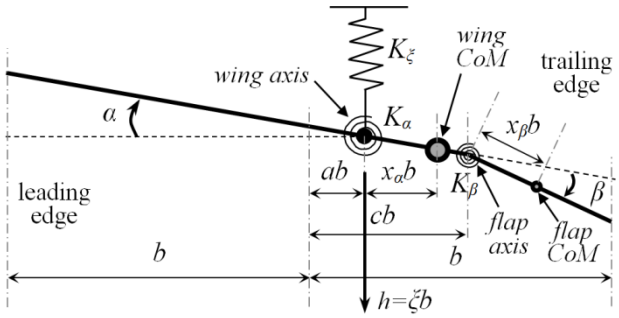

Fig. 1 Schematic of aeroelastic model showing displacements and parameters

This particular model is appropriate for demonstration of the present objective as it models the dynamics of the actuator, the means through which the input will be applied. This is important because of the non-smooth inputs that are required, and takes into account the fact that it is never possible in the real world to implement non-smooth motions.

B. Nonlinear model

A nonlinear term is now introduced into the pitch degree of freedom of the model in eq (7). The resulting system may be expressed as

$$\dot{\mathbf{x}} = \underline{\mathbf{f}}(\mathbf{x}) + \underline{\mathbf{g}}(\mathbf{x})u\,, \quad \text{where } \underline{\mathbf{f}}(\mathbf{x}) = \begin{Bmatrix} \dot{\mathbf{q}} \\ \boldsymbol{\Psi}\mathbf{q} + \boldsymbol{\Phi}\dot{\mathbf{q}} + \boldsymbol{\Lambda}\mathbf{q}_a + \boldsymbol{\Omega}\mathbf{f}_{nl} \\ \mathbf{E}_1\mathbf{q} + \mathbf{E}_2\dot{\mathbf{q}} + \mathbf{F}_p\mathbf{q}_a \end{Bmatrix}, \quad \underline{\mathbf{g}}(\mathbf{x}) = \begin{bmatrix} \mathbf{0} \\ \boldsymbol{\Pi} \\ \mathbf{0} \end{bmatrix}, \tag{8}$$

$$\boldsymbol{\Psi} = -\mathbf{M}_t^{-1}\mathbf{K}_t\,, \quad \boldsymbol{\Phi} = -\mathbf{M}_t^{-1}\mathbf{C}_t\,, \quad \boldsymbol{\Omega} = -\mathbf{M}_t^{-1}\,, \quad \boldsymbol{\Pi} = \mathbf{M}_t^{-1}\mathbf{G}\,, \quad \boldsymbol{\Lambda} = \mathbf{M}_t^{-1}\mathbf{D}\,.$$

In the present case $\underline{\mathbf{g}}(\mathbf{x}) \equiv \mathbf{B}$ and the use of different symbols is aimed at maintaining conventionally accepted notation in the linear and affine nonlinear cases. Note that the system has the special structure mentioned in section II.B earlier, notwithstanding the additional augmented states in this model. It is now necessary to express the pitch

non-smooth nonlinearity through the nonlinear force vector $\mathbf{f}_{nl}$. A possible choice of the underlying linear system is one whose pitch stiffness is equal to the slope of the outer regions in the freeplay/piece-wise linear cases. In this case, the nonlinear force vector may be expressed as

$$\mathbf{f}_{nl} = \begin{cases} -\lambda \Delta \mathbf{K}_s \mathbf{q}, & |\alpha| \le g_\alpha \\ -\lambda \Delta \mathbf{K}_s \mathbf{g}_\alpha, & \alpha > g_\alpha \\ \lambda \Delta \mathbf{K}_s \mathbf{g}_\alpha, & \alpha < -g_\alpha \end{cases} \qquad \mathbf{g}_\alpha = \begin{cases} 0 \\ g_\alpha \\ 0 \end{cases}, \tag{9}$$

$$\lambda \le 1, \qquad \Delta \mathbf{K}_s = K_\alpha \mathbf{e}_2 \mathbf{e}_2^T, \qquad \mathbf{e}_2 = \mathbf{I}_{3_{(:,2)}},$$

where $\lambda, g_\alpha, K_\alpha$ are the parameters describing the non-smooth nonlinearity, defined in Table 1. Setting $\lambda = 1$ produces the freeplay case, whereas any other value subject to the constraint $\lambda \le 1$ produces a piece-wise linear nonlinearity. An example of the pitch moment profile for pitch freeplay and piecewise linear pitch stiffness is depicted by the solid line in Fig. 2.

Table 1 Nonlinearity parameters for the non-smooth pitch stiffness

Parameter	Description
g_α	initial (lower) stiffness region on either side of $\alpha = 0^\circ$
λ	$K_{\alpha_{(\lvert\alpha\rvert \le g_\alpha)}} = (1-\lambda) K_\alpha$, where $K_{\alpha_{(\lvert\alpha\rvert \le g_\alpha)}}$ is the initial (lower) stiffness
K_α	stiffness in outer regions ($\lvert\alpha\rvert > g_\alpha$), chosen as the pitch stiffness K_α of the desired linear system

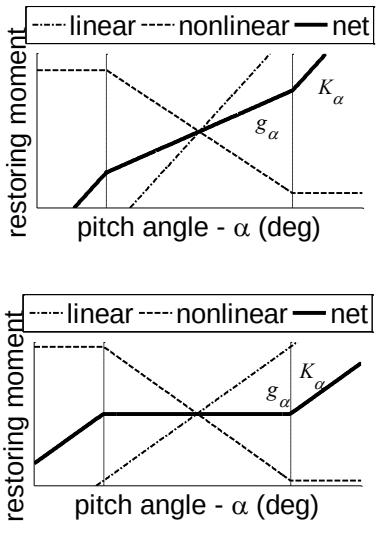

Fig. 2 Pitch moment profile in the presence of pitch piece-wise linear stiffness/pitch freeplay

The non-smooth nature of the freeplay/piece-wise linear nonlinearity would result in non-smooth but continuous forces and accelerations. However, the resulting changes in all states of the system will be C^1 smooth (i.e. continuously differentiable, having continuous but non-smooth derivatives), as they are obtained as time-integrals of the accelerations.

C. Input-output linearisation

The classical input-output linearisation approach introduced earlier is now followed to apply feedback linearisation by controlling the plunge displacement. The co-ordinates of the linear system become

$$z_1 = y = x_1\,, \qquad z_2 = \dot{y} = \dot{x}_1 = x_4 \tag{10}$$

from eq. (7). Here, the output y is chosen as the plunge displacement $\xi = x_1$. The partially linearised system may then be obtained as

$$\begin{Bmatrix} \dot{z}_1 \\ \dot{z}_2 \end{Bmatrix} = \begin{bmatrix} 0 & 1 \\ 0 & 0 \end{bmatrix} \begin{Bmatrix} z_1 \\ z_2 \end{Bmatrix} + \begin{bmatrix} 0 \\ 1 \end{bmatrix} \bar{u}\,, \qquad \bar{u} = \underline{\mathbf{f}}\left(\mathbf{x}\right)_{(4)} + \varpi_1 u, \qquad \mathbf{\Pi} = \left\{ \varpi_1 \quad \varpi_2 \quad \varpi_3 \right\}^T, \tag{11}$$

with $\bar{u}$ being an artificial input associated with the linearised system. An appropriate choice for $\bar{u}$ can be made depending on the control requirement. In the present work it is desired to apply pole-placement and thereby prescribe a new natural frequency ω_n and damping ratio ζ_n of a chosen decoupled subsystem, which can be achieved by setting

$$\bar{u} = -\omega_n^2 z_1 - 2\zeta_n \omega_n z_2 \quad \text{to give the closed-loop system} \quad \begin{Bmatrix} \dot{z}_1 \\ \dot{z}_2 \end{Bmatrix} = \begin{bmatrix} 0 & 1 \\ -\omega_n^2 & -2\zeta_n\omega_n \end{bmatrix} \begin{Bmatrix} z_1 \\ z_2 \end{Bmatrix}. \tag{12}$$

Since there remains an un-linearised set of six states, it is necessary to examine the zero-dynamics to ensure their stability when designing a controller. Expressions for the remaining linear co-ordinates are first required to complete the transformation. These are chosen as

$$z_3 = x_2, \quad z_4 = x_3 + \varpi_2 x_4 - \varpi_1 x_5, \quad z_5 = \varpi_3 x_4 - \varpi_1 x_6,$$
$$z_6 = \varpi_3 x_5 - \varpi_2 x_6, \quad z_7 = x_7, \quad z_8 = x_8, \tag{13}$$

completing the full 8×8 transformation from nonlinear to linear co-ordinates as $\mathbf{z} = \mathbf{T}\mathbf{x}$. This particular choice ensures that the input terms do not appear in the internal dynamics, as is desirable. The resulting zero-dynamics are found as

$$\dot{\mathbf{z}}_{(3:8)_{ZD}} = \begin{pmatrix} \left[\mathbf{T}_{(3:8,:)}\mathbf{A}\left(\mathbf{T}^{-1}\right)_{(:,3:8)}\right]\mathbf{z}_{(3:8)_{ZD}} \\ +\left[\mathbf{T}_{(3:8,:)}\boldsymbol{\theta}\right]\psi\left(z_3\right) \end{pmatrix}, \quad \boldsymbol{\theta} = -\lambda K_\alpha \begin{bmatrix} \mathbf{0}_{(3\times1)} \\ \boldsymbol{\Omega}\mathbf{e}_2 \\ \mathbf{0}_{(2\times1)} \end{bmatrix}, \quad \psi\left(z_3\right) = \begin{cases} z_3, & |z_3| \le g_\alpha \\ g_\alpha, & z_3 > g_\alpha \\ -g_\alpha, & z_3 < -g_\alpha \end{cases} \tag{14}$$

and where the matrix $\mathbf{A}$ is given in eq. (7). Thus, one is able to investigate the stability of the zero-dynamics for a given set of system parameters from (14). Such an investigation is undertaken in the numerical simulation.

IV. Numerical Simulations

In this section, results from numerical simulation of the aeroservoelastic system described in section III.A will be presented. Initially, appropriate values for the parameters of a linear system will be set, after which the symmetric freeplay/piece-wise linear nonlinearity described in section III.B will be incorporated. The final part of this section will then demonstrate the application of feedback linearisation for the pole-placement control objective outlined in section III.C.

A. Parameters of aeroservoelastic system

The parameter values presented in Table 2 are representative of a real 2 degree of freedom linear aeroservoelastic wind-tunnel model being used at the University of Liverpool. Most values were obtained during experiments conducted by Papatheou et al. [25]. The values for ω_β, r_β were chosen to have appropriate magnitudes relative to the remaining parameters.

Table 2 Parameters of the linear aeroservoelastic system

Parameter	Value	Parameter	Value	Parameter	Value
ω_α (rad/s)	35.354	c	0.5428	ω_β (rad/s)	100
r_α	0.4	b (m)	0.175	r_β	0.079057
x_α	0.09	μ	69.0	x_β	0.0125
ω_ξ (rad/s)	22.948	ζ_ξ	0.002	ζ_β	0.002
a	-0.33333	ζ_α	0.015		

It is found that the linear flutter speed of this system is U^*= 2.793. A plot showing the frequency domain behaviour with varying airspeed may be found in [26].

B. Time-domain response of uncontrolled nonlinear system

The nonlinear model described in section III.B is now simulated, for the cases of (a) freeplay and (b) piece-wise linear stiffness. In both cases, the gap of the initial regime is set to $g_\alpha = \pm 1^\circ$. In the piece-wise linear case λ is set to 0.6. The parameters of the target linear system are set to the values given in Table 2; thus, the slope of the outer regions will be $K_\alpha = r_\alpha^2 \omega_\alpha^2$. The reduced air speed is chosen as $U^* = 2.0$. Initial values for plunge and pitch are arbitrarily set to $\xi = 0.01,\ \alpha = 3^\circ$ respectively, and zero for all other states. No prescribed or external excitation is introduced to the system. The resulting structural responses are shown in Fig. 3.

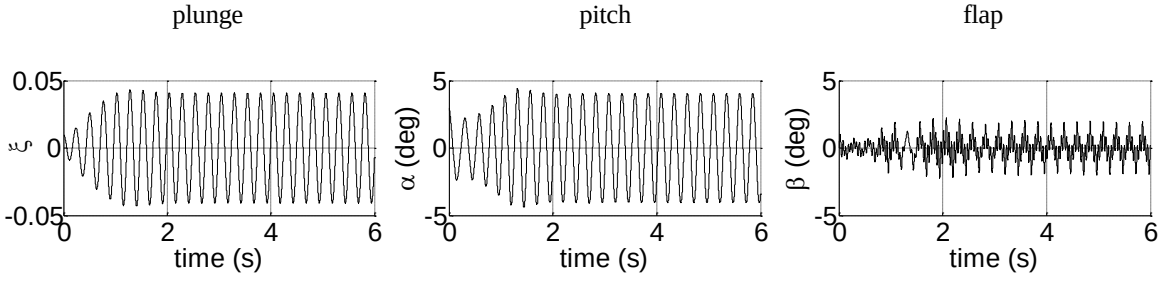

(a) freeplay

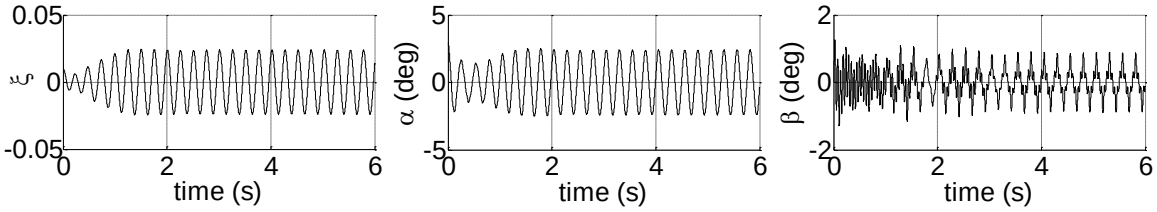

(b) piece-wise linear stiffness

Fig. 3 Structural states of nonlinear system at *U=2.0**

It is evident that the response settles into a limit cycle oscillation in both cases, which occurs at an airspeed that is less than the LFS $U^* = 2.793$. An important step in numerically simulating the piece-wise linear system is locating accurately the switching points between the different regimes of the nonlinearity. An adaptation of Henon's method [27] was used in [28] to achieve this task, and has been employed in the present work for the same purpose.

C. Stability of the zero-dynamics

The zero-dynamics expressed in eq. (14) in section III.C are now analysed for both (a) freeplay and (b) piece-wise linear stiffness. An analytical formulation for studying stability based on Lyapunov theory is provided in Appendix A3. The analysis starts by expressing the zero-dynamics (14) compactly as

$$\dot{\underset{\sim}{\mathbf{z}}} = \hat{\mathbf{A}}\underset{\sim}{\mathbf{z}} + \hat{\mathbf{b}}\psi\left(z_3\right) = \underset{\sim}{\mathbf{f}}\left(\underset{\sim}{\mathbf{z}}, t\right). \tag{15}$$

The numerical value of the Hurwitz matrix $\hat{\mathbf{A}}$ and the vector $\hat{\mathbf{b}}$ (different for freeplay and piece-wise linear cases) in the present example are given in Appendix A4. It can be shown that the equilibrium points of the zero-dynamics can obtained by solving

$$\begin{aligned} &\hat{\mathbf{A}}\underset{\sim}{\mathbf{z}}_{eq} + \hat{\mathbf{b}}z_3 = \mathbf{0}, \quad |z_3| \le g_\alpha \\ &\hat{\mathbf{A}}\underset{\sim}{\mathbf{z}}_{eq} + \hat{\mathbf{b}}g_\alpha = \mathbf{0}, \quad z_3 > g_\alpha \\ &\hat{\mathbf{A}}\underset{\sim}{\mathbf{z}}_{eq} - \hat{\mathbf{b}}g_\alpha = \mathbf{0}, \quad z_3 < -g_\alpha. \end{aligned} \tag{16}$$

(see Appendix A3). The stability of the equilibrium points was studied using the aforementioned Lyapunov theory. To solve the LMIs arising in the associated numerical computations, the Yalmip [29] and Sedumi [30] Matlab toolboxes were employed.

Freeplay case:

In the case of the trivial equilibrium, it was not possible to find an arbitrary matrix $\mathbf{P} \succ 0$ (such that $V = \frac{1}{2}\underset{\sim}{\mathbf{z}}^T \mathbf{P} \underset{\sim}{\mathbf{z}} > 0$) that results in $\mathbf{P}\left(\hat{\mathbf{A}} + \hat{\mathbf{b}}\mathbf{p}^T\right) \prec 0$ (such that $\dot{V} < 0$), as required by Lyapunov theory ($\succ, \prec$ denote positive/negative definiteness respectively). However, it was possible to find a suitable matrix $\mathbf{P}$ in the case of the non-trivial equilibria (see Appendix A4 for numerical value). Fig. 4 shows a collection of simulated time-domain responses of the zero-dynamics, each with a randomly generated initial condition (the figures show the response as they approach steady-state, after the initial transients have largely decayed).

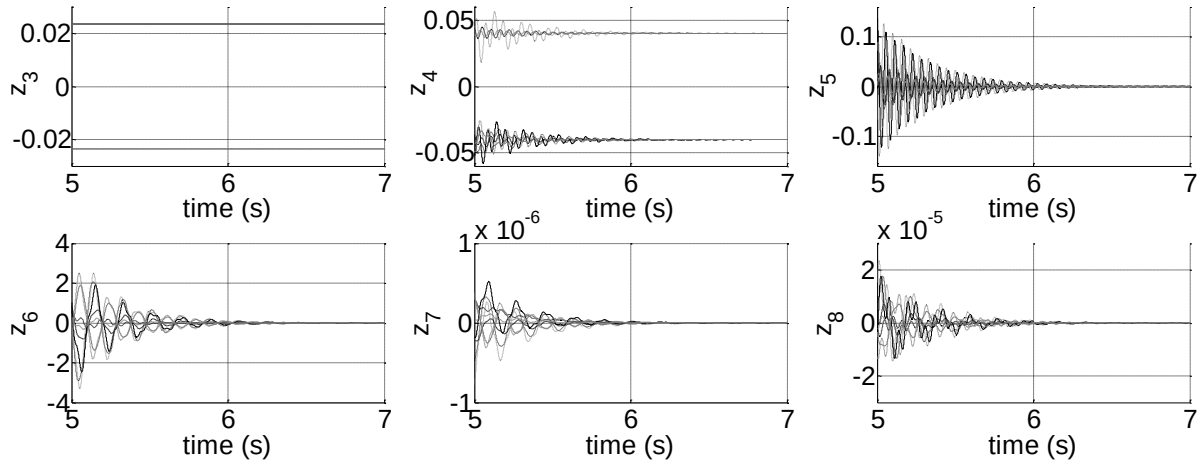

Fig. 4 Zero-dynamics for freeplay case, as steady-state is reached (several simulation results plotted together)

Note that none of the responses converge to the origin. This is a reflection of the fact that it is not possible to find a $\mathbf{P} \succ 0$ that results in $\mathbf{P}\left(\hat{\mathbf{A}} + \hat{\mathbf{b}}\mathbf{p}^T\right)$ being negative definite. This appears to be a clear indication that this particular equilibrium point is unstable. This happens to agree with intuition, as one would not expect a settled state

within a region of zero pitch stiffness ($|z_3| \leq g_\alpha$). It can be seen that in all cases the responses settle to one of the two non-zero equilibria. This is directly related to the fact that one is able to satisfy the $\mathbf{P}\hat{\mathbf{A}} \prec 0$ condition simultaneously with $\mathbf{P} \succ 0$, indicating asymptotic stability of these equilibria.

It is of interest to gain some understanding of the basin of attraction of the non-trivial equilibria. One reason as to why this may be useful is to shed light on the possibility of a response establishing a pseudo-stable trajectory about the origin, such as a limit cycle oscillation. Analytical and numerical studies were carried out (see Appendix A3), and results showed that any solution within $|z_3| \leq g_\alpha$ will lie within the basin of attraction of both non-zero equilibria. Thus, it has to be the case that such solutions will be attracted by one non-zero equilibrium or the other, precluding the possibility of a pseudo-stable oscillation.

Piece-wise linear case:

The equilibrium points in this case may be computed as previously using eq. (16). It transpires that the solutions to the second and third equations are not feasible, as they violate the $z_3 > g_\alpha$ and $z_3 < -g_\alpha$ conditions respectively. Thus, in the piece-wise linear case, one is left with a single equilibrium point, obtained by solving the first equation in eq. (16). In doing so, the resulting matrix $\left(\hat{\mathbf{A}} + \hat{\mathbf{b}}\mathbf{p}^T\right)$ turns out to be full-rank, resulting in the solution being the trivial equilibrium $\underset{\sim}{\mathbf{z}}_{eq} = \mathbf{0}$. Using Lyapunov theory, the problem now reduces to finding a $\mathbf{P} \succ 0$ that results in $\mathbf{P}\left(\hat{\mathbf{A}} + \hat{\mathbf{b}}\mathbf{p}^T\right)$ being negative definite. Such a $\mathbf{P}$ was successfully found (whereas in the freeplay case this was not possible), thus proving the asymptotic stability of the trivial equilibrium (numerical value of $\mathbf{P}$ is provided in Appendix A4). This conclusion is supported by the results from numerical simulations presented in Fig. 5, which shows several simulation results plotted together, each simulated with a different initial condition generated randomly. The convergence of the zero-dynamics to the origin is clearly visible.

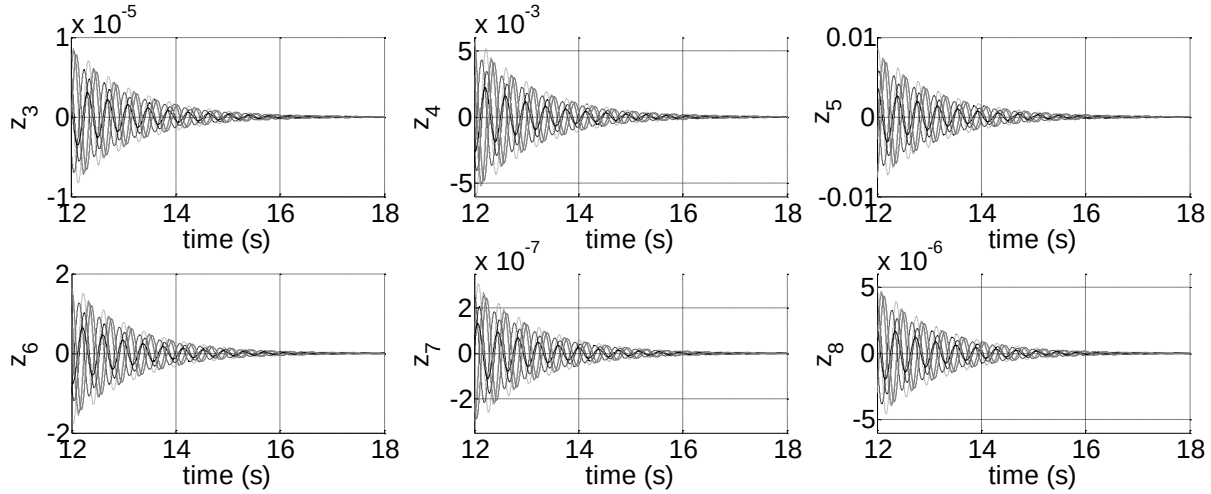

Fig. 5 Zero-dynamics for piece-wise linear case, as steady-state is reached (several simulation results plotted together)

D. Time-domain response of closed-loop system with feedback linearisation

The existence of asymptotic stable equilibria of the zero-dynamics has been shown in the preceding section. Thus, it is now possible to proceed with the application of the chosen feedback linearising control. Plunge-output feedback linearisation with pole-placement, as described in section III.C is now carried out in both the freeplay and piecewise linear stiffness cases. The target natural frequency and damping ratio are chosen as $\omega_{n_\xi} = 1\text{Hz}, \zeta_{n_\xi} = 0.1$, respectively. The resulting closed-loop response, for the same initial conditions as the open-loop case, is shown in Fig. 6.

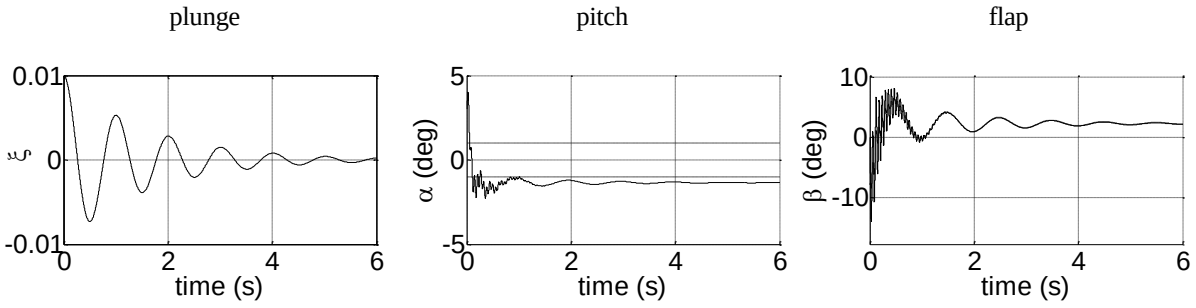

(a) freeplay

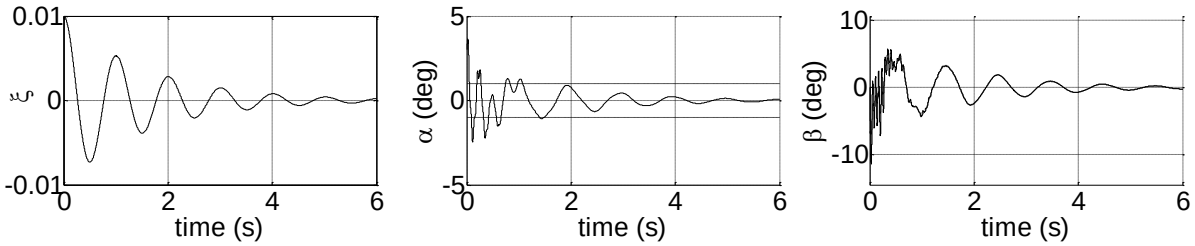

(b) piece-wise linear stiffness

Fig. 6 Closed-loop response of system at *U=2.0**

It is evident from the first subplots in both (a) and (b) that the target natural frequency of 1 Hz is achieved in the plunge motion, as expected. The pitch motion in (a), confined to the internal dynamics settles down to a non-zero stable equilibrium close to the lower bound of the freeplay gap ±1° (indicated by the dashed horizontal lines), as seen in the middle plot (this result is expected, in view of the nature of the zero-dynamics equilibrium points studied earlier). The pitch motion may settle down to either the upper or lower freeplay bound depending on the initial condition. In the piece-wise linear case (b), the pitch motion and also other responses converge to zero, as expected from the nature of the zero-dynamics. The actual flap motion is given in the final subplot in both cases. This is compared against the commanded input in Fig. 7, where the difference between the two is clearer.

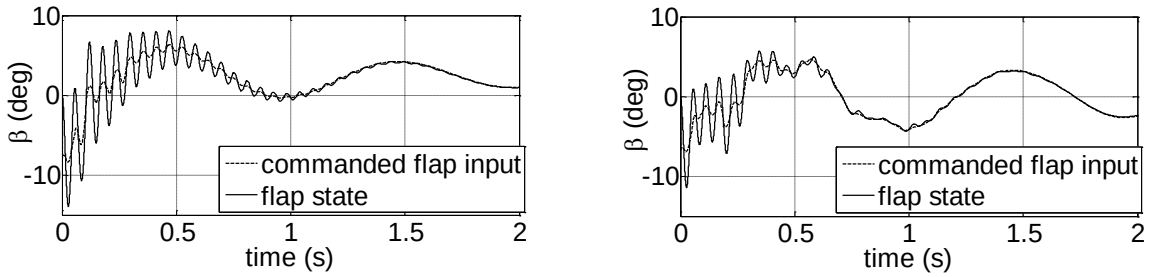

(a) freeplay

(b) piece-wise linear stiffness

Fig. 7 Comparing commanded and actual flap angles *U=2.0**

Closer inspection of the input reveals non-smooth changes corresponding to the switching points in the non-smooth pitch stiffness. This is expected, as the input is designed to cancel the system dynamics which include the non-smooth forcing terms. Since the dynamics of the actuator have been modelled, the input takes into account

what the actuator is physically capable of achieving, and therefore its non-smooth nature will not degrade feedback linearisation that is based on a nonlinear control law derived from the model. Thus, exact pole placement will be achieved in the absence of nonlinearity parameter errors.

A similar approach was followed with the pitch displacement chosen as the output. In this case, it transpired that the zero-dynamics were unstable for both freeplay and piece-wise linear stiffness, indicating that this configuration of input-output linearisation is not feasible.

V. Conclusion

In this article, the authors have demonstrated the application of feedback linearisation in systems having a non-smooth structural nonlinearity that is part of the state. A careful examination of the underlying theory shows that a relaxation of the smoothness conditions required in feedback linearisation in the general case is possible for the class of second-order dynamical systems considered due to its special structure in the state-space representation; this in turn permits the use of feedback linearisation when the plant is beset by a non-smooth or even discontinuous nonlinearity. An in-depth analysis of the stability of the zero-dynamics arising from plunge-output linearisation has been carried out, where the feasibility of feedback linearisation has been demonstrated. A description of the expected linearised dynamics has been provided, where it is pointed out that in partial feedback linearisation the system may suffer non-smooth dynamics if the nonlinearity is discontinuous. It is hoped that the clarity shed by this work on the issue of non-smooth feedback linearisation encourages further research that combines feedback linearisation methods with non-smooth nonlinear systems.

Appendices

A1 System matrices for aeroelastic model

The approximated 8-state unsteady aeroelastic model developed by Edwards et al. has been employed in this work. The matrices in the state-space model and related expressions are given in this section for the convenience of the reader, but may also be found in [23], [31].

The structural and aerodynamic inertia matrices respectively are given by

$$\mathbf{M}_s = \begin{bmatrix} 1 & x_\alpha & x_\beta \\ x_\alpha & r_\alpha^2 & r_\beta^2 + (c-a)x_\beta \\ x_\beta & r_\beta^2 + (c-a)x_\beta & r_\beta^2 \end{bmatrix}, \qquad \mathbf{M}_{nc} = \begin{bmatrix} \pi & -\pi a & -T_1 \\ -\pi a & \pi\left(\frac{1}{8} + a^2\right) & 2T_{13} \\ -T_1 & 2T_{13} & -\frac{1}{\pi}T_3 \end{bmatrix}, \quad \text{(A1-1)}$$

the structural and aerodynamic damping matrices respectively by

$$\mathbf{C}_s = \mathbf{V}^{-T} \begin{bmatrix} 2m_h\zeta_h\omega_h & 0 & 0 \\ 0 & 2m_\alpha\zeta_\alpha\omega_\alpha & 0 \\ 0 & 0 & 2m_\beta\zeta_\beta\omega_\beta \end{bmatrix} \mathbf{V}^{-1}, \quad \text{(A1-2)}$$

$$\mathbf{C}_{nc} = \begin{bmatrix} 0 & \pi & -T_4 \\ 0 & \pi\left(\frac{1}{2} - a\right) & \left(T_1 - T_8 + \frac{1}{2}T_{11} - (c-a)T_4\right) \\ 0 & \left(-2T_9 - T_1 + T_4\left(a - \frac{1}{2}\right)\right) & -\frac{1}{2\pi}T_4T_{11} \end{bmatrix},$$

and the structural and aerodynamic stiffness matrices respectively by

$$\mathbf{K}_s = \begin{bmatrix} \omega_h^2 & 0 & 0 \\ 0 & r_\alpha^2\omega_\alpha^2 & 0 \\ 0 & 0 & r_\beta^2\omega_\beta^2 \end{bmatrix}, \qquad \mathbf{K}_{nc} = \begin{bmatrix} 0 & 0 & 0 \\ 0 & 0 & \left(T_4 + T_{10}\right) \\ 0 & 0 & \frac{1}{\pi}\left(T_5 - T_4T_{10}\right) \end{bmatrix}. \quad \text{(A1-3)}$$

The state-space form of the system (in the absence of any nonlinearities), including the two additional aerodynamic states is then obtained using eq. (7). The quantities appearing in this equation are:

$$\mathbf{M}_t = \mathbf{M}_s + \eta \mathbf{M}_{nc}\,, \qquad \mathbf{C}_t = \mathbf{C}_s + \eta\left(U^*\omega_\alpha\right)\left(\mathbf{C}_{nc} - \tfrac{1}{2}\mathbf{R}\mathbf{S}_2\right),$$

$$\mathbf{K}_t = \mathbf{K}_s + \eta\left(U^*\omega_\alpha\right)^2\left(\mathbf{K}_{nc} - \tfrac{1}{2}\mathbf{R}\mathbf{S}_1\right), \quad \mathbf{D} = \eta\left(U^*\omega_\alpha\right)^2 \mathbf{R}\left[\,0.006825\left(U^*\omega_\alpha\right) \quad 0.10805\right],$$

$$\mathbf{E}_1 = \left(U^*\omega_\alpha\right)\begin{bmatrix}\mathbf{0}_{(1\times 3)}\\ \\ \mathbf{S}_1\end{bmatrix}, \quad \mathbf{E}_2 = \begin{bmatrix}\mathbf{0}_{(1\times 3)}\\ \\ \mathbf{S}_2\end{bmatrix}, \quad \mathbf{F}_p = \begin{bmatrix} 0 & 1 \\ \\ -0.01365\left(U^*\omega_\alpha\right)^2 & -0.3455\left(U^*\omega_\alpha\right)\end{bmatrix}, \tag{A1-4}$$

$$\mathbf{R} = \left[-2\pi \quad 2\pi\left(a+\tfrac{1}{2}\right) \quad -T_{12}\right]^T, \quad \mathbf{S}_1 = \left[0 \quad 1 \quad \tfrac{1}{\pi}T_{10}\right], \qquad \mathbf{S}_2 = \left[1 \quad \left(\tfrac{1}{2}-a\right) \quad \tfrac{1}{2\pi}T_{11}\right],$$

$$\eta = 1/\pi\mu, \qquad U^*\omega_\alpha = U/b\,.$$

The various "*T*" functions defined by Theodorsen [24] appearing in this section are also given here for the convenience of the reader.

$$T_1 = -\tfrac{1}{3}\sqrt{1-c^2}\left(2+c^2\right) + c\cos^{-1}c\,,$$

$$T_3 = -\left(\tfrac{1}{8}+c^2\right)\left(\cos^{-1}c\right)^2 + \tfrac{1}{4}c\sqrt{1-c^2}\left(\cos^{-1}c\right)\left(7+2c^2\right) - \tfrac{1}{8}\left(1-c^2\right)\left(5c^2+4\right),$$

$$T_4 = -\left(\cos^{-1}c\right) + c\sqrt{1-c^2}\,, \quad T_5 = -\left(1-c^2\right) - \left(\cos^{-1}c\right)^2 + 2c\sqrt{1-c^2}\left(\cos^{-1}c\right),$$

$$T_7 = -\left(\tfrac{1}{8}+c^2\right)\left(\cos^{-1}c\right) + \tfrac{1}{8}c\sqrt{1-c^2}\left(7+2c^2\right), \quad T_8 = -\tfrac{1}{3}\sqrt{1-c^2}\left(2c^2+1\right) + c\cos^{-1}c\,,$$

$$T_9 = \tfrac{1}{2}\left[\tfrac{1}{3}\left(\sqrt{1-c^2}\right)^3 + aT_4\right], \quad T_{10} = \sqrt{1-c^2} + \cos^{-1}c\,,$$

$$T_{11} = \left(\cos^{-1}c\right)\left(1-2c\right) + \sqrt{1-c^2}\left(2-c\right), \quad T_{12} = \sqrt{1-c^2}\left(2+c\right) - \left(\cos^{-1}c\right)\left(2c+1\right),$$

$$T_{13} = \tfrac{1}{2}\left[-T_7 - \left(c-a\right)T_1\right]. \tag{A1-5}$$

A2 Input-output linearisation in a general nonlinear system

Consider the following nonlinear system without the special structure discussed in section II.A earlier.

$$\dot{x}_1 = a\sin x_2 + f_{nl}\left(x_2\right), \qquad \dot{x}_2 = -x_1^2 + u, \qquad y = x_1, \tag{A2-1}$$

where $f_{nl}\left(x_2\right)$ is a non-smooth nonlinearity, the computation of the co-ordinate transformation results in

$$\begin{aligned} z_1 &= y = x_1 & z_2 &= \dot{y} = \dot{x}_1 = a\sin x_2 + f_{nl}\left(x_2\right) \\ \dot{z}_1 &= \dot{x}_1 = a\sin x_2 + f_{nl}\left(x_2\right) & \dot{z}_2 &= \ddot{x}_1 = \left(a\cos x_2 + \tfrac{d}{dx_2}\left(f_{nl}\right)\right)\left(-x_1^2 + u\right) \end{aligned}, \tag{A2-2}$$

and it is evident that differentiation of the non-smooth term is required in obtaining the linear dynamics, and therefore the transformation $\mathbf{z} = \mathbf{T}\left(\mathbf{x}\right)$ is not continuously differentiable. Thus, this configuration of input-output feedback linearisation is not feasible.

A3 Stability of the plunge zero-dynamics

The nonlinear force vector in eq. (9) may be expressed as a function of z_3, concisely, as

$$\mathbf{f}_{nl} = -\lambda K_\alpha \mathbf{e}_2 \psi\left(z_3\right) \quad \text{where} \quad \psi\left(z_3\right) = \begin{cases} z_3, & \left|z_3\right| \le g_\alpha \\ g_\alpha, & z_3 > g_\alpha \\ -g_\alpha, & z_3 < -g_\alpha \end{cases} \quad \text{and} \quad \mathbf{e}_2 = \mathbf{I}_{3_{(:,2)}}. \tag{A3-1}$$

Combining this representation of $\mathbf{f}_{nl}$ with eq. (14), and denoting $\underset{\sim}{\mathbf{z}} = \mathbf{z}_{(3:8)_{ZD}}$, the zero-dynamics may be expressed in the form

$$\dot{\underset{\sim}{\mathbf{z}}} = \widehat{\mathbf{A}}\underset{\sim}{\mathbf{z}} + \widehat{\mathbf{b}}\psi\left(z_3\right) = \underset{\sim}{\mathbf{f}}\left(\underset{\sim}{\mathbf{z}}, t\right). \tag{A3-2}$$

The equilibrium points of the system are found from

$$\widehat{\mathbf{A}}\underset{\sim}{\mathbf{z}}_{eq} + \widehat{\mathbf{b}}\psi\left(z_3\right) = \mathbf{0}, \tag{A3-3}$$

so in each of the 3 conditions,

$$\begin{aligned} \hat{\mathbf{A}}\underset{\sim}{\mathbf{z}}_{eq} + \hat{\mathbf{b}}z_3 &= \mathbf{0}, \quad |z_3| \le g_\alpha \\ \hat{\mathbf{A}}\underset{\sim}{\mathbf{z}}_{eq} + \hat{\mathbf{b}}g_\alpha &= \mathbf{0}, \quad z_3 > g_\alpha \\ \hat{\mathbf{A}}\underset{\sim}{\mathbf{z}}_{eq} - \hat{\mathbf{b}}g_\alpha &= \mathbf{0}, \quad z_3 < -g_\alpha. \end{aligned} \tag{A3-4}$$

Using the substitution

$$z_3 = \mathbf{p}^T\underset{\sim}{\mathbf{z}}, \qquad \mathbf{p} = \begin{bmatrix} 1 & 0 & 0 & 0 & 0 & 0 \end{bmatrix}^T, \tag{A3-5}$$

the first line of (A3-4) may be simplified,

$$\begin{aligned} \left(\hat{\mathbf{A}} + \hat{\mathbf{b}}\mathbf{p}^T\right)\underset{\sim}{\mathbf{z}}_{eq} &= \mathbf{0}, \quad |z_3| \le g_\alpha \\ \hat{\mathbf{A}}\underset{\sim}{\mathbf{z}}_{eq} + \hat{\mathbf{b}}g_\alpha &= \mathbf{0}, \quad z_3 > g_\alpha \\ \hat{\mathbf{A}}\underset{\sim}{\mathbf{z}}_{eq} - \hat{\mathbf{b}}g_\alpha &= \mathbf{0}, \quad z_3 < -g_\alpha. \end{aligned} \tag{A3-6}$$

For non-singular $\hat{\mathbf{A}}$ and $\left(\hat{\mathbf{A}} + \hat{\mathbf{b}}\mathbf{p}^T\right)$, the solutions are found as

$$\underset{\sim}{\mathbf{z}}_{eq} = \begin{cases} \mathbf{0}, & |z_3| \le g_\alpha \\ -\hat{\mathbf{A}}^{-1}\hat{\mathbf{b}}g_\alpha, & z_3 > g_\alpha \\ \hat{\mathbf{A}}^{-1}\hat{\mathbf{b}}g_\alpha, & z_3 < -g_\alpha. \end{cases} \tag{A3-7}$$

Since the zero-dynamics being analysed are non-smooth, it may be inadequate to apply smooth stability theory in a piece-wise manner. A general Lyapunov approach for analysing the stability of non-smooth systems

is given in [32], and will be employed for the present task. If the equilibrium point of interest were simply $\underset{\sim}{\mathbf{z}}_{eq} = \mathbf{0}$, one can choose as a Lyapunov function

$$V = \tfrac{1}{2}\underset{\sim}{\mathbf{z}}^T \mathbf{P} \underset{\sim}{\mathbf{z}}, \qquad \mathbf{P} \succ 0, \qquad \mathbf{P} = \mathbf{P}^T, \tag{A3-8}$$

where $\mathbf{P}$ is arbitrary, and $\succ$ denotes positive-definiteness. However, since one also has two non-zero equilibria in addition to the trivial equilibrium, the origin should be redefined such that the Lyapunov function is based around a given equilibrium point, viz.,

$$\begin{aligned} \hat{\underset{\sim}{\mathbf{z}}} &= \underset{\sim}{\mathbf{z}} - \underset{\sim}{\mathbf{z}}_{eq} \\ V &= \tfrac{1}{2}\hat{\underset{\sim}{\mathbf{z}}}^T \mathbf{P} \hat{\underset{\sim}{\mathbf{z}}}, \qquad \mathbf{P} \succ 0, \qquad \mathbf{P} = \mathbf{P}^T. \end{aligned} \tag{A3-9}$$

The dynamics in the new variable would be

$$\dot{\hat{\underset{\sim}{\mathbf{z}}}} = \dot{\underset{\sim}{\mathbf{z}}} - \dot{\underset{\sim}{\mathbf{z}}}_{eq} = \dot{\underset{\sim}{\mathbf{z}}} = \underset{\sim}{\mathbf{f}}\left(\underset{\sim}{\mathbf{z}}, t\right) = \underset{\sim}{\mathbf{f}}\left(\hat{\underset{\sim}{\mathbf{z}}} + \underset{\sim}{\mathbf{z}}_{eq}, t\right) =: \underset{\sim}{\mathbf{g}}\left(\hat{\underset{\sim}{\mathbf{z}}}, t\right), \tag{A3-10}$$

$$\underset{\sim}{\mathbf{g}}\left(\hat{\underset{\sim}{\mathbf{z}}}, t\right) = \hat{\mathbf{A}}\hat{\underset{\sim}{\mathbf{z}}} + \hat{\mathbf{A}}\underset{\sim}{\mathbf{z}}_{eq} + \hat{\mathbf{b}}\psi\left(z_3\right). \tag{A3-11}$$

Note that the Lyapunov function in (A3-9) is smooth (the only exception to this is when the nonlinearity is discontinuous, in which case the velocity would be non-smooth but continuous, causing the Lyapunov function to be non-smooth. This scenario will not be considered in the present paper). The stability theory in [32] is used to express the derivative of the Lyapunov function as

$$\dot{\tilde{V}} = \bigcap_{\xi \in \partial V} \xi^T K\left[\underset{\sim}{\mathbf{g}}\left(\hat{\underset{\sim}{\mathbf{z}}}, t\right)\right], \tag{A3-12}$$

where ∂V is Clarke's generalised gradient and $K[\ ]$ denotes the Filippov differential inclusion. Since V is smooth,

$$\partial V = \nabla V, \qquad \nabla V = \frac{\partial V}{\partial \hat{\underset{\sim}{\mathbf{z}}}} = \mathbf{P}\hat{\underset{\sim}{\mathbf{z}}}, \tag{A3-13}$$

leading to

$$\dot{\hat{V}} = \nabla V^T K\left[\underset{\sim}{\mathbf{g}}\left(\hat{\underset{\sim}{\mathbf{z}}}, t\right)\right]. \tag{A3-14}$$

Utilising Theorems 1 – 5 and 7 in [33], $K\left[\underset{\sim}{\mathbf{g}}\left(\hat{\underset{\sim}{\mathbf{z}}}, t\right)\right]$ is computed as

$$K\left[\underset{\sim}{\mathbf{g}}\left(\hat{\underset{\sim}{\mathbf{z}}}, t\right)\right] = K\left[\hat{\mathbf{A}}\hat{\underset{\sim}{\mathbf{z}}} + \hat{\mathbf{A}}\underset{\sim}{\mathbf{z}}_{eq} + \hat{\mathbf{b}}\psi\left(z_3\right)\right] = \hat{\mathbf{A}}\hat{\underset{\sim}{\mathbf{z}}} + \hat{\mathbf{A}}\underset{\sim}{\mathbf{z}}_{eq} + \hat{\mathbf{b}}K\left[\psi\left(z_3\right)\right] \tag{A3-15}$$

since $\hat{\mathbf{A}}\hat{\underset{\sim}{\mathbf{z}}}$ and $\hat{\mathbf{b}}$ are continuous and $\underset{\sim}{\mathbf{z}}_{eq}$ is constant for a given equilibrium point. Substituting from (A3-13), (A3-15) into (A3-14),

$$\dot{\hat{V}} = \hat{\underset{\sim}{\mathbf{z}}}^T \mathbf{P}\left(\hat{\mathbf{A}}\hat{\underset{\sim}{\mathbf{z}}} + \hat{\mathbf{A}}\underset{\sim}{\mathbf{z}}_{eq} + \hat{\mathbf{b}}K\left[\psi\left(z_3\right)\right]\right)$$

$$K\left[\psi\left(z_3\right)\right] = \begin{cases} z_3, & \left|z_3\right| \le g_\alpha \\ g_\alpha, & z_3 > g_\alpha \\ -g_\alpha, & z_3 < -g_\alpha. \end{cases} \tag{A3-16}$$

For the three conditions, with substitutions made from (A3-5) and (A3-9), this may be expressed as

$$\dot{\tilde{V}} = \begin{cases} \hat{\underset{\sim}{\mathbf{z}}}^T \mathbf{P}\left(\hat{\mathbf{A}} + \hat{\mathbf{b}}\mathbf{p}^T\right)\left(\hat{\underset{\sim}{\mathbf{z}}} + \underset{\sim}{\mathbf{z}}_{eq}\right), & |z_3| \le g_\alpha \\ \hat{\underset{\sim}{\mathbf{z}}}^T \mathbf{P}\left(\hat{\mathbf{A}}\hat{\underset{\sim}{\mathbf{z}}} + \hat{\mathbf{A}}\underset{\sim}{\mathbf{z}}_{eq} + \hat{\mathbf{b}}g_\alpha\right), & z_3 > g_\alpha \\ \hat{\underset{\sim}{\mathbf{z}}}^T \mathbf{P}\left(\hat{\mathbf{A}}\hat{\underset{\sim}{\mathbf{z}}} + \hat{\mathbf{A}}\underset{\sim}{\mathbf{z}}_{eq} - \hat{\mathbf{b}}g_\alpha\right), & z_3 < -g_\alpha. \end{cases} \tag{A3-17}$$

From Lyapunov theory, one requires the derivatives in eq. (A3-17) to be strictly negative for asymptotic stability. These expressions need to be analysed with respect to each of the three equilibrium points in eq. (A3-7) to determine the stability of the system in each of the three regions of z_3; thus, a total of nine expressions arise. After some simplification, these can be shown to be:

Equilibrium point $\underset{\sim}{\mathbf{z}}_{eq} = \mathbf{0}$

$$\begin{aligned} &(a) \quad \hat{\underset{\sim}{\mathbf{z}}}^T \mathbf{P}\left(\hat{\mathbf{A}} + \hat{\mathbf{b}}\mathbf{p}^T\right)\hat{\underset{\sim}{\mathbf{z}}} < 0, \quad |z_3| \le g_\alpha \\ &(b) \quad \hat{\underset{\sim}{\mathbf{z}}}^T \mathbf{P}\hat{\mathbf{A}}\hat{\underset{\sim}{\mathbf{z}}} + \hat{\underset{\sim}{\mathbf{z}}}^T \mathbf{P}\hat{\mathbf{b}}g_\alpha < 0 \quad z_3 > g_\alpha \\ &(c) \quad \hat{\underset{\sim}{\mathbf{z}}}^T \mathbf{P}\hat{\mathbf{A}}\hat{\underset{\sim}{\mathbf{z}}} - \hat{\underset{\sim}{\mathbf{z}}}^T \mathbf{P}\hat{\mathbf{b}}g_\alpha < 0 \quad z_3 < -g_\alpha. \end{aligned} \tag{A3-18}$$

Equilibrium point $\underset{\sim}{\mathbf{z}}_{eq} = -\hat{\mathbf{A}}^{-1}\hat{\mathbf{b}}g_\alpha$

$$\begin{aligned} &(a) \quad \hat{\underset{\sim}{\mathbf{z}}}^T \mathbf{P}\left(\hat{\mathbf{A}} + \hat{\mathbf{b}}\mathbf{p}^T\right)\hat{\underset{\sim}{\mathbf{z}}} - \hat{\underset{\sim}{\mathbf{z}}}^T \mathbf{P}\hat{\mathbf{b}}\left(1 + \mathbf{p}^T\hat{\mathbf{A}}^{-1}\hat{\mathbf{b}}\right)g_\alpha < 0, \quad |z_3| \le g_\alpha \\ &(b) \quad \hat{\underset{\sim}{\mathbf{z}}}^T \mathbf{P}\hat{\mathbf{A}}\hat{\underset{\sim}{\mathbf{z}}} < 0, \quad z_3 > g_\alpha \\ &(c) \quad \hat{\underset{\sim}{\mathbf{z}}}^T \mathbf{P}\hat{\mathbf{A}}\hat{\underset{\sim}{\mathbf{z}}} - 2\hat{\underset{\sim}{\mathbf{z}}}^T \mathbf{P}\hat{\mathbf{b}}g_\alpha < 0, \quad z_3 < -g_\alpha. \end{aligned} \tag{A3-19}$$

Equilibrium point $\underset{\sim}{\mathbf{z}}_{eq} = \hat{\mathbf{A}}^{-1}\hat{\mathbf{b}}g_\alpha$

$$
\begin{aligned}
&(a) \quad \hat{\underset{\sim}{\mathbf{z}}}^T\mathbf{P}\left(\hat{\mathbf{A}}+\hat{\mathbf{b}}\mathbf{p}^T\right)\hat{\underset{\sim}{\mathbf{z}}}+\hat{\underset{\sim}{\mathbf{z}}}^T\mathbf{P}\hat{\mathbf{b}}\left(1+\mathbf{p}^T\hat{\mathbf{A}}^{-1}\hat{\mathbf{b}}\right)g_\alpha<0, \quad |z_3|\le g_\alpha \\
&(b) \quad \hat{\underset{\sim}{\mathbf{z}}}^T\mathbf{P}\hat{\mathbf{A}}\hat{\underset{\sim}{\mathbf{z}}}+2\hat{\underset{\sim}{\mathbf{z}}}^T\mathbf{P}\hat{\mathbf{b}}g_\alpha<0, \quad z_3>g_\alpha \\
&(c) \quad \hat{\underset{\sim}{\mathbf{z}}}^T\mathbf{P}\hat{\mathbf{A}}\hat{\underset{\sim}{\mathbf{z}}}<0, \quad z_3<-g_\alpha.
\end{aligned}
\tag{A3-20}
$$

The task now is to verify whether the set of three inequalities pertaining to each equilibrium point can be satisfied. If a given inequality can be satisfied, that would signify that the respective equilibrium point can attract a general point located in the region pertaining to the inequality. As a starting point, one may consider the stability of each equilibrium point in its own region, namely by analysing equations (A3-18)a, (A3-19)b and (A3-20)c. For stability, it is required that $\mathbf{P}\left(\hat{\mathbf{A}}+\hat{\mathbf{b}}\mathbf{p}^T\right)\prec 0$ in the first case and $\mathbf{P}\hat{\mathbf{A}}\prec 0$ in the remaining two cases ($\prec$ denotes negative-definiteness).

Now consider the equilibrium $\underset{\sim}{\mathbf{z}}_{eq}=-\hat{\mathbf{A}}^{-1}\hat{\mathbf{b}}g_\alpha$. Eq. (A3-19)a describes how this equilibrium attracts points in the centre region $|z_3|\le g_\alpha$. Combining this with equations (A3-5) and (A3-9) and simplifying leads to

$$
\hat{\underset{\sim}{\mathbf{z}}}^T\mathbf{P}\hat{\mathbf{A}}\hat{\underset{\sim}{\mathbf{z}}}+\hat{\underset{\sim}{\mathbf{z}}}^T\mathbf{P}\hat{\mathbf{b}}\left(z_3-g_\alpha\right)<0, \quad |z_3|\le g_\alpha. \tag{A3-21}
$$

It should always be possible to satisfy the negative definiteness of the first term for Hurwitz $\hat{\mathbf{A}}$. Also, by definition $\left(z_3-g_\alpha\right)$ in the range $|z_3|\le g_\alpha$ is either negative or zero. Therefore, *a possible* solution to the above equation is

$$
\left(\hat{\mathbf{b}}^T\mathbf{P}\right)\hat{\underset{\sim}{\mathbf{z}}}=\varepsilon, \quad \varepsilon\ge 0, \quad |z_3|\le g_\alpha. \tag{A3-22}
$$

In this case, a general expression for $\hat{\underset{\sim}{\mathbf{z}}}$ will be

$$
\hat{\underset{\sim}{\mathbf{z}}}=\hat{\underset{\sim}{\mathbf{z}}}_{mn}+\mathbf{Z}_{\left(\hat{\mathbf{b}}^T\mathbf{P}\right)}\mathbf{w}, \quad |z_3|\le g_\alpha, \tag{A3-23}
$$

where

$$\hat{\underset{\sim}{\mathbf{z}}}_{mn} = \left(\mathbf{P}\hat{\mathbf{b}}\right)\left[\left(\hat{\mathbf{b}}^T\mathbf{P}\right)\left(\mathbf{P}\hat{\mathbf{b}}\right)\right]^{-1}\varepsilon = \underset{\sim}{\mathbf{m}}\varepsilon \tag{A3-24}$$

is the minimum-norm solution to (A3-22), $\mathbf{Z}_{\left(\hat{\mathbf{b}}^T\mathbf{P}\right)}$ is the null-space matrix of $\hat{\mathbf{b}}^T\mathbf{P}$ and $\mathbf{w}$ is an arbitrary vector. It is not clear at this stage whether subsequent values of $\hat{\underset{\sim}{\mathbf{z}}}$ will continue to obey eq. (A3-23) and thus have guaranteed asymptotic stability. This is because in the present expression, one does not have the quadratic form usually associated with Lyapunov stability. Combining this solution with the zero-dynamics will shed light on this problem.

Equations (A3-1), (A3-11), (A3-24), (A3-23), $\underset{\sim}{\mathbf{z}}_{eq} = -\hat{\mathbf{A}}^{-1}\hat{\mathbf{b}}g_\alpha$ are combined with the time-derivative of eq. (A3-23), and simplified to obtain the dynamics of the parameter vector $\mathbf{w}$ for a fixed value of the bound ε, viz.,

$$\dot{\mathbf{w}} = \left(\mathbf{Z}^T_{\left(\hat{\mathbf{b}}^T\mathbf{P}\right)}\left(\hat{\mathbf{A}} + \hat{\mathbf{b}}\mathbf{p}^T\right)\mathbf{Z}_{\left(\hat{\mathbf{b}}^T\mathbf{P}\right)}\right)\mathbf{w} + \mathbf{Z}^T_{\left(\hat{\mathbf{b}}^T\mathbf{P}\right)}\begin{pmatrix} -\hat{\mathbf{b}}\left(1+\mathbf{p}^T\hat{\mathbf{A}}^{-1}\hat{\mathbf{b}}\right)g_\alpha \\ \\ \left(\hat{\mathbf{A}} + \hat{\mathbf{b}}\mathbf{p}^T\right)\underset{\sim}{\mathbf{m}}c_3 \end{pmatrix}, \quad |z_3| \le g_\alpha. \tag{A3-25}$$

One may conclude from the above equation that since any solution $\hat{\underset{\sim}{\mathbf{z}}}$ is bound by the zero-dynamics, all parameter vectors $\mathbf{w}$ must necessarily obey the trajectory defined by eq. (A3-25), which is stable provided the matrix $\mathbf{Z}^T_{\left(\hat{\mathbf{b}}^T\mathbf{P}\right)}\left(\hat{\mathbf{A}} + \hat{\mathbf{b}}\mathbf{p}^T\right)\mathbf{Z}_{\left(\hat{\mathbf{b}}^T\mathbf{P}\right)}$ is Hurwitz. This can be said of the various $\mathbf{w}$ for all possible values ε. This leads one to conclude that if a solution $\hat{\underset{\sim}{\mathbf{z}}}$ satisfies (A3-23) at a given time, it will continue to do so for all future time. Using symmetry, a very similar approach can be used to draw conclusions regarding stability with respect to the other non-zero equilibrium.

The above analysis has focused on studying the basin of attraction of $\underset{\sim}{\mathbf{z}}_{eq} = -\hat{\mathbf{A}}^{-1}\hat{\mathbf{b}}g_\alpha$ whilst remaining oblivious to the remaining non-zero equilibrium point, namely $\underset{\sim}{\mathbf{z}}_{eq} = \hat{\mathbf{A}}^{-1}\hat{\mathbf{b}}g_\alpha$. From a similar analysis to that above, it can be shown that the region $|z_3| \le g_\alpha$ belongs also to the basin of attraction of this equilibrium point. In fact, further analytical expressions (coupled with numerical simulations) – omitted here for brevity – show that any solution satisfying (A3-19)a also satisfies (A3-20)a. This leads to the conclusion that instances of $\hat{\underset{\sim}{\mathbf{z}}}$ satisfying $|z_3| \le g_\alpha$ may be attracted by either of the non-trivial equilibria.

Note that the above analysis has provided a formula for a general point $\hat{\underset{\sim}{\mathbf{z}}}$, which provides a sufficient condition for the point to be attracted by either of the non-zero equilibria. It is acknowledged that not all instances of $\hat{\underset{\sim}{\mathbf{z}}}$ will necessarily conform to this solution form. The authors have gained ample confidence through comprehensive numerical tests that the general case of $\hat{\underset{\sim}{\mathbf{z}}}$ will also always be within the basin of attraction of (at least one) of the non-zero equilibria, and therefore be attracted by one of them in all cases.

A4 Numerical values of matrices

The matrices $\hat{\mathbf{A}}, \hat{\mathbf{b}}, \mathbf{P}$ pertaining to the numerical simulation in section IV are

$$\hat{\mathbf{A}} = \begin{bmatrix} \mathbf{a}_1 & \mathbf{a}_2 & \mathbf{a}_3 & \mathbf{a}_4 & \mathbf{a}_5 & \mathbf{a}_6 \end{bmatrix}, \quad \text{where}$$

$$\mathbf{a}_1 = \begin{Bmatrix} 0 \\ -1.052519802118332e+05 \\ 5.399869146317270e+05 \\ -1.659823663570565e+07 \\ 0 \\ 7.070800000000000e+01 \end{Bmatrix}, \quad \mathbf{a}_2 = \begin{Bmatrix} 0 \\ 4.041090088153123e+04 \\ -4.298752404294511e+05 \\ -1.728568173261333e+06 \\ 0 \\ 4.134300537289159e+01 \end{Bmatrix}, \quad \mathbf{a}_3 = \begin{Bmatrix} -2.570282306800488e-03 \\ 4.272077768816730e+03 \\ -4.545223216288383e+04 \\ -1.830205646000262e+05 \\ 0 \\ 4.371383129559804e+00 \end{Bmatrix}$$

$$\mathbf{a}_4 = \begin{Bmatrix} 7.060748738249028e-05 \\ -1.171834173862442e+02 \\ 1.246584721963058e+03 \\ 5.013723978938279e+03 \\ 0 \\ -1.199639476900394e-01 \end{Bmatrix}, \quad \mathbf{a}_5 = \begin{Bmatrix} 0 \\ 1.244850769997651e+05 \\ -1.132149605329264e+06 \\ 1.667116413208036e+06 \\ 0 \\ -6.824483025360000e+01 \end{Bmatrix}, \quad \mathbf{a}_6 = \begin{Bmatrix} 0 \\ 2.787217464100848e+04 \\ -2.534879865121954e+05 \\ 3.732669082569129e+05 \\ 1.000000000000000e+00 \\ -2.442961400000000e+01 \end{Bmatrix}. \quad \text{(A4-1)}$$

Freeplay case:

$$\hat{\mathbf{b}} = \begin{bmatrix} 0 \\ 2.342301136732328e+05 \\ -1.712999346432723e+06 \\ 1.832552450362287e+07 \\ 0 \\ 0 \end{bmatrix}, \quad \text{(A4-2)}$$

$$\mathbf{P} = \begin{bmatrix} \mathbf{p}_1 & \mathbf{p}_2 & \mathbf{p}_3 & \mathbf{p}_4 & \mathbf{p}_5 & \mathbf{p}_6 \end{bmatrix}, \quad \text{where}$$

$$\mathbf{p}_1 = \begin{Bmatrix} 9.372607855313569e\text{-}01 \\ 8.740468264190424e\text{-}02 \\ 9.234713203835910e\text{-}03 \\ -2.538207346361724e\text{-}04 \\ -4.870521398378206e\text{-}02 \\ -2.158444391650875e\text{-}03 \end{Bmatrix}, \quad \mathbf{p}_2 = \begin{Bmatrix} 8.740468264190424e\text{-}02 \\ 1.836685287561729e\text{-}02 \\ 1.941132661625013e\text{-}03 \\ -5.324019202272837e\text{-}05 \\ 1.615430260018339e\text{-}02 \\ 3.820056422105477e\text{-}03 \end{Bmatrix}, \quad \mathbf{p}_3 = \begin{Bmatrix} 9.234713203835910e\text{-}03 \\ 1.941132661625013e\text{-}03 \\ 2.051524045951996e\text{-}04 \\ -5.626781131016655e\text{-}06 \\ 1.706849539147576e\text{-}03 \\ 4.036721215201463e\text{-}04 \end{Bmatrix}$$

$$\mathbf{p}_4 = \begin{Bmatrix} -2.538207346361724e\text{-}04 \\ -5.324019202272837e\text{-}05 \\ -5.626781131016655e\text{-}06 \\ 1.543320242320278e\text{-}07 \\ -4.671170920817329e\text{-}05 \\ -1.103599334489257e\text{-}05 \end{Bmatrix}, \quad \mathbf{p}_5 = \begin{Bmatrix} -4.870521398378206e\text{-}02 \\ 1.615430260018339e\text{-}02 \\ 1.706849539147576e\text{-}03 \\ -4.671170920817329e\text{-}05 \\ 3.164968847347670e\text{-}01 \\ 1.088581433922096e\text{-}02 \end{Bmatrix}, \quad \mathbf{p}_6 = \begin{Bmatrix} -2.158444391650875e\text{-}03 \\ 3.820056422105477e\text{-}03 \\ 4.036721215201463e\text{-}04 \\ -1.103599334489257e\text{-}05 \\ 1.088581433922096e\text{-}02 \\ 5.402751369202207e\text{-}03 \end{Bmatrix}. \quad \text{(A4-3)}$$

Piece-wise linear case:

$$\hat{\mathbf{b}} = \begin{bmatrix} 0 \\ 1.405380682039397e+05 \\ -1.027799607859634e+06 \\ 1.099531470217372e+07 \\ 0 \\ 0 \end{bmatrix}, \quad \text{(A4-4)}$$

$$\mathbf{P} = \begin{bmatrix} \mathbf{p}_1 & \mathbf{p}_2 & \mathbf{p}_3 & \mathbf{p}_4 & \mathbf{p}_5 & \mathbf{p}_6 \end{bmatrix}, \quad \text{where}$$

$$\mathbf{p}_1 = \begin{Bmatrix} 5.056526725019898\text{e-}01 \\ 1.462612920992349\text{e-}01 \\ 1.545870907700230\text{e-}02 \\ -4.241601950240046\text{e-}04 \\ 1.772732012964278\text{e-}01 \\ 4.624078483505167\text{e-}02 \end{Bmatrix}, \quad \mathbf{p}_2 = \begin{Bmatrix} 1.462612920992349\text{e-}01 \\ 9.720189272664394\text{e-}02 \\ 1.027518723239798\text{e-}02 \\ -2.818129594597023\text{e-}04 \\ 2.032449173738622\text{e-}01 \\ 4.334432088729381\text{e-}02 \end{Bmatrix}, \quad \mathbf{p}_3 = \begin{Bmatrix} 1.545870907700230\text{e-}02 \\ 1.027518723239798\text{e-}02 \\ 1.086191397194798\text{e-}03 \\ -2.979037465256925\text{e-}05 \\ 2.147300258521749\text{e-}02 \\ 4.578753780004211\text{e-}03 \end{Bmatrix}$$

$$\mathbf{p}_4 = \begin{Bmatrix} -4.241601950240046\text{e-}04 \\ -2.818129594597023\text{e-}04 \\ -2.979037465256925\text{e-}05 \\ 8.170553983314395\text{e-}07 \\ -5.886465972362083\text{e-}04 \\ -1.254781254657852\text{e-}04 \end{Bmatrix}, \quad \mathbf{p}_5 = \begin{Bmatrix} 1.772732012964278\text{e-}01 \\ 2.032449173738622\text{e-}01 \\ 2.147300258521749\text{e-}02 \\ -5.886465972362083\text{e-}04 \\ 7.070018043909696\text{e-}01 \\ 1.341051528474015\text{e-}01 \end{Bmatrix}, \quad \mathbf{p}_6 = \begin{Bmatrix} 4.624078483505167\text{e-}02 \\ 4.334432088729381\text{e-}02 \\ 4.578753780004211\text{e-}03 \\ -1.254781254657852\text{e-}04 \\ 1.341051528474015\text{e-}01 \\ 3.323272777784759\text{e-}02 \end{Bmatrix}. \quad \text{(A4-5)}$$

Acknowledgements

The authors gratefully acknowledge the support of the Engineering and Physical Sciences Research Council (EPSRC) grant EP/J004987/1 on Nonlinear Active Vibration Suppression in Aeroelasticity.

References

[1] *Springer Handbook of Robotics*: Springer, 2008.

[2] te Braake, H. A. B., van Can, E. J. L., Scherpen, J. M. A., and Verbruggen, H. B. "Control of nonlinear chemical processes using neural models and feedback linearization," *Computers & Chemical Engineering*, Vol. 22, No. 7–8, 1998, pp. 1113-1127.

doi: http://dx.doi.org/10.1016/S0098-1354(97)00267-6

[3] Isidori, A. *Nonlinear Control Systems*. Berlin Heidelberg New York: Springer, 1995.

[4] Khalil, H. K. *Nonlinear Systems*: Prentice Hall, 2002.

[5] Nijmeijer, H., and Schaft, A. v. d. *Nonlinear dynamical control systems*: Springer-Verlag New York, Inc., 1990.

[6] Platanitis, G., and Strganac, T. W. "Control of a nonlinear wing section using leading- and trailing-edge surfaces," *Journal of Guidance Control and Dynamics*, Vol. 27, No. 1, 2004, pp. 52-58.

doi: 10.2514/1.9284

[7] Strganac, T., Ko, J., and Thompson, D. "Identification and control of limit cycle oscillations in aeroelastic systems," *Journal of Guidance Control and Dynamics*, Vol. 23, No. 6, 2000, pp. 1127-1133.

[8] Ko, J., Strganac, T. W., and Kurdila, A. J. "Adaptive Feedback Linearization for the Control of a Typical Wing Section with Structural Nonlinearity," *Nonlinear Dynamics*, Vol. 18, No. 3, 1999, pp. 289-301.

doi: 10.1023/a:1008323629064

[9] Jiffri, S., Paoletti, P., Cooper, J. E., and Mottershead, J. E. "Feedback Linearisation for Nonlinear Vibration Problems," *Shock and Vibration*, Vol. Vol. 2014, Article ID 106531, 2014.

doi: 10.1155/2014/106531

[10] Jiffri, S., Mottershead, J. E., and Cooper, J. E. "Adaptive Feedback Linearisation and Control of a Flexible Aircraft Wing," *Topics in Modal Analysis, Volume 7, Proceedings of the 31st IMAC, A Conference on Structural Dynamics*, Orange County CA, USA, 2013, pp. 683-699.

[11] Jiffri, S., Mottershead, J. E., and Cooper, J. E. "Active Control of a Nonlinear Flexible Aircraft Wing," *International Conference on Structural Engineering Dynamics*, Sesimbra, Portugal, 2013.

[12] Jiffri, S., Mottershead, J. E., and Cooper, J. E. "Nonlinear Control of a Flexible Aeroelastic System," *International Forum on Aeroelasticity & Structural Dynamics*, Bristol Marriott Royal Hotel, Bristol, UK, 2013.

[13] Recker, D. A., Kokotovic, P. V., Rhode, D., and Winkelman, J. "Adaptive Nonlinear Control of Systems containing a Deadzone," *Proceedings of the 30th IEEE Conference on Decision and Control, Vols 1-3*, New York, 1991, pp. 2111-2115.

[14] Ma, X. L., and Tao, G. "Adaptive actuator compensation control with feedback linearization," *IEEE Transactions on Automatic Control*, Vol. 45, No. 9, 2000, pp. 1705-1710.
doi: 10.1109/9.880627

[15] Sun, Z. D., and Ge, S. S. "Nonregular feedback linearization: A nonsmooth approach," *IEEE Transactions on Automatic Control*, Vol. 48, No. 10, 2003, pp. 1772-1776.
doi: 10.1109/tac.2003.817914

[16] Hatipoglu, C., and Ozguner, U. "Controller design for a class of systems with inherent right hand side discontinuities," *Proceedings of the 36th IEEE Conference on Decision and Control, Vols 1-5*. IEEE, New York, 1997, pp. 4024-4025.

[17] Hatipoglu, C., Ozguner, U., and Amer Automat Control, C. "Robust control of systems involving non-smooth nonlinearities using modified sliding manifolds," *Proceedings of the 1998 American Control Conference, Vols 1-6*. IEEE, New York, 1998, pp. 2133-2137.

[18] Tao, G. "Adaptive control of systems with nonsmooth input and output nonlinearities," *IEEE Transactions on Automatic Control*, Vol. 41, No. 9, 1996, pp. 1348-1352.

[19] Tao, G., and Kokotovic, P. V. "Adaptive control of systems with unknown non-smooth non-linearities," *International Journal of Adaptive Control and Signal Processing*, Vol. 11, No. 1, 1997, pp. 81-100.
doi: 10.1002/(sici)1099-1115(199702)11:1<81::aid-acs396>3.0.co;2-a

[20] Lin, W., and Qian, C. J. "Adaptive control of nonlinearly parameterized systems: A nonsmooth feedback framework," *IEEE Transactions on Automatic Control*, Vol. 47, No. 5, 2002, pp. 757-774.

[21] Ma, H.-J., and Yang, G.-H. "Adaptive output control of uncertain nonlinear systems with non-symmetric dead-zone input," *Automatica*, Vol. 46, No. 2, 2010, pp. 413-420.

doi: http://dx.doi.org/10.1016/j.automatica.2009.11.010

[22] Zhou, J., and Wen, C. Y. "Adaptive Backstepping Control of Uncertain Systems: Nonsmooth Nonlinearities, Interactions or Time-Variations," *Adaptive Backstepping Control of Uncertain Systems: Nonsmooth Nonlinearities, Interactions or Time-Variations*. Vol. 372, Springer-Verlag Berlin, Berlin, 2008.

[23] Edwards, J. W., Ashley, H., and Breakwell, J. V. "Unsteady aerodynamic modeling for arbitrary motions," *AIAA Journal*, Vol. 17, No. 4, 1979, pp. 365-374.

doi: 10.2514/3.7348

[24] Theodorsen, T. "General theory of aerodynamic instability and the mechanism of flutter," *NACA Report no. 496*, 1935, pp. 413-433.

[25] Papatheou, E., Tantaroudas, N. D., Da Ronch, A., Badcock, K., Mottershead, J. E., and Cooper, J. E. "Active Control for Flutter Suppression: An Experimental Investigation," *International Forum on Aeroelasticity and Structural Dynamics (IFASD)*, Bristol, UK, 24-26 June, 2013.

[26] Jiffri, S., and Mottershead, J. E. "Nonlinear control of an aeroelastic system with a non-smooth structural nonlinearity," *VETOMAC-X 2014*, University of Manchester, UK.

[27] Henon, M. "On the numerical computation of Poincaré maps," *Physica D: Nonlinear Phenomena*, Vol. 5, No. 2–3, 1982, pp. 412-414.

doi: http://dx.doi.org/10.1016/0167-2789(82)90034-3

[28] Conner, M. D., Virgin, L. N., and Dowell, E. H. "Accurate numerical integration of state-space models for aeroelastic systems with free play," *AIAA Journal*, Vol. 34, No. 10, 1996, pp. 2202-2205.

doi: 10.2514/3.13377

[29] Loefberg, J. "Automatic robust convex programming," *Optimization Methods & Software*, Vol. 27, No. 1, 2012, pp. 115-129.

doi: 10.1080/10556788.2010.517532

[30] Sturm, J. F. "Using SeDuMi 1.02, a MATLAB toolbox for optimization over symmetric cones," *Optimization Methods & Software*, Vol. 11-2, No. 1-4, 1999, pp. 625-653.

doi: 10.1080/10556789908805766

[31] Li, D., Guo, S., and Xiang, J. "Aeroelastic dynamic response and control of an airfoil section with control surface nonlinearities," *Journal of Sound and Vibration*, Vol. 329, No. 22, 2010, pp. 4756-4771.

doi: 10.1016/j.jsv.2010.06.006

[32] Shevitz, D., and Paden, B. "Lyapunov stability theory of nonsmooth systems," *IEEE Transactions on Automatic Control*, Vol. 39, No. 9, 1994, pp. 1910-1914.

doi: 10.1109/9.317122

[33] Paden, B. E., and Sastry, S. S. "A calculus for computing Filippov differential inclusion with application to the variable structure control of robot manipulators," *IEEE Transactions on Circuits and Systems*, Vol. 34, No. 1, 1987, pp. 73-82.

doi: 10.1109/tcs.1987.1086038